



ATTRIBUTION OF CHANGES IN SMALL AND LARGE FLOODS ACROSS BRAZIL

Gabriel Anzolin¹; Vinícius B. P. Chagas¹; Pedro L. B. Chaffe²

¹Graduate Program of Environmental Engineering, Federal University of Santa Catarina, Florianópolis, Brazil.

5 ²Department of Sanitary and Environmental Engineering, Federal University of Santa Catarina, Florianópolis, Brazil.

Corresponding author: Gabriel Anzolin (gabriel_anzolin@hotmail.com).

Abstract. In tropical regions, flood changes are driven by a combination of event rainfall characteristics and antecedent wetness changes. However, how the interactions between storage capacity, event rainfall, and antecedent wetness influence flood changes across event magnitudes is elusive. Here, we explore the causes of changes in small and large floods by combining flood elasticities with trends in event rainfall peak and pre-event antecedent wetness of 765 catchments in Brazil. Our results suggest that large floods are increasing more than small ones, corresponding to 80% of substantial flood increases. While those changes in large events are usually rainfall-driven, changes in small floods are mostly aligned with changes in antecedent wetness. We find that in regions with high water storage capacity, antecedent wetness drives changes in both small and large floods. Conversely, in regions with low water storage capacity, changes in small floods are driven by antecedent wetness, whereas large floods are mainly rainfall-driven, as rainfall outweighs antecedent wetness in those fast-saturating catchments. Our findings highlight that reliable predictions of flood responses to climate change should account for both event magnitude and catchment storage capacities, as climatic drivers alone are insufficient to fully explain flood changes.

1 Introduction

20 The frequency and magnitude of river flooding have remarkably changed worldwide over the recent decades (Do et al., 2017; Gudmundsson et al., 2021; Slater et al., 2021; Wasko et al., 2021). Detection and attribution of flood changes usually rely on the analysis of average floods, thus assuming that changes are independent of flood magnitude (e.g., Bertola et al., 2019; Blöschl et al., 2019; Chagas et al., 2022b). However, the interplay between water storage capacity, event rainfall, and antecedent wetness conditions is likely to drive changes in small and large events differently (Bertola et al., 2020; Sharma et al., 2018; Slater and Villarini, 2016; Wasko and Nathan, 2019).

In Europe, changes in small and large floods exhibit distinct spatial patterns (Bertola et al., 2020); even though those changes are generally driven by a single mechanism across flood magnitudes (Bertola et al., 2021). For instance, in Northwestern



Europe, both small and large floods are primarily rainfall-driven, whereas in Eastern Europe, flood changes are linked to snowmelt processes (Bertola et al., 2020, 2021). In Australia and Bavaria, there is a threshold beyond which flood change
30 becomes independent of antecedent wetness, i.e., larger floods are driven by changes in extreme rainfall (Brunner et al., 2021; Wasko and Nathan, 2019). This finding has been confirmed on a global scale across different climate regimes, with changes in large floods mostly associated with changes in rainfall rather than antecedent wetness (Wasko et al., 2021).

A key limitation in flood change attribution is that most assessments have been conducted in temperate-dominated climates, which differ substantially from tropical regions in terms of rainfall regimes, evaporation rates, and water storage dynamics
35 (Minasny and Hartemink, 2011; Wohl et al., 2012). These notable differences pose challenges for generalizing flood change mechanisms across event magnitudes to tropical climates. In Brazil, changes in large floods have been mostly analyzed in global assessments that include a limited number of catchments and disregard local effects (Wasko et al., 2021). As a tropical region, Brazil offers a valuable opportunity for large-scale investigation of how the interactions between water storage capacity, event rainfall, and antecedent wetness influence flood changes across event magnitudes.

40 Here, we aim to explore the causes of changes in small and large flood events by combining flood elasticities with trends in rainfall and antecedent wetness of 765 catchments in Brazil. For each catchment, we select flood peaks, their corresponding rainfall peaks, and antecedent wetness using a frequency-based peak-over-threshold approach. The detection and attribution of flood changes are investigated by combining event-scale flood elasticities and trends in driving mechanisms using a multivariate quantile regression framework.

45 2 Material and Methods

2.1 Study area and data

We use daily streamflow data of 765 catchments across Brazil from the Brazilian National Water Agency (<http://www.snirh.gov.br/hidroweb/>), as made available by the Brazilian version of the Catchment Attributes and Meteorology for Large-Sample Studies (CAMELS-BR; Chagas et al., 2020). The data period ranges from 1980 to 2018, which represents a
50 trade-off between data availability in terms of record length and spatial coverage. We select only high-quality data based on data availability and catchment characteristics as follows: (i) at least 20 water years (starting in September) without any data gap; (ii) records without spurious values such as incorrect order of magnitude or zeros in place of missing data; (iii) catchments with low reservoir influence, characterized by less than 30% of artificial streamflow regulation, calculated as the ratio of total reservoir storage to annual streamflow. Fig. 1a shows the spatial distribution of the selected streamflow gauges, classified into
55 four hotspots: Amazon (AM), North (N), Southeast (SE), and South (S). The hotspots represent regions for which flood changes are particularly clear, and flood processes are broadly similar, based on previous assessments of flood changes (Chagas



et al., 2022b), and flood mechanisms (Chagas et al., 2022a). The sizes of the selected catchments span approximately five orders of magnitude, ranging from about 10^1 to 10^6 km 2 , with a median size close to 10^3 km 2 (Fig. 1b).

We use daily catchment-average precipitation from the Climate Hazards Group InfraRed Precipitation with Station data (CHIRPS v2.0; Funk et al., 2015), also as made available in CAMELS-BR dataset. The data period is from 1981 to 2018, with a spatial resolution of 0.05° (approximately 5.5 km). We use the CHIRPS dataset because, compared to other precipitation products, it corresponds better with observed precipitation and flood change in Brazil (Chagas et al., 2022b).

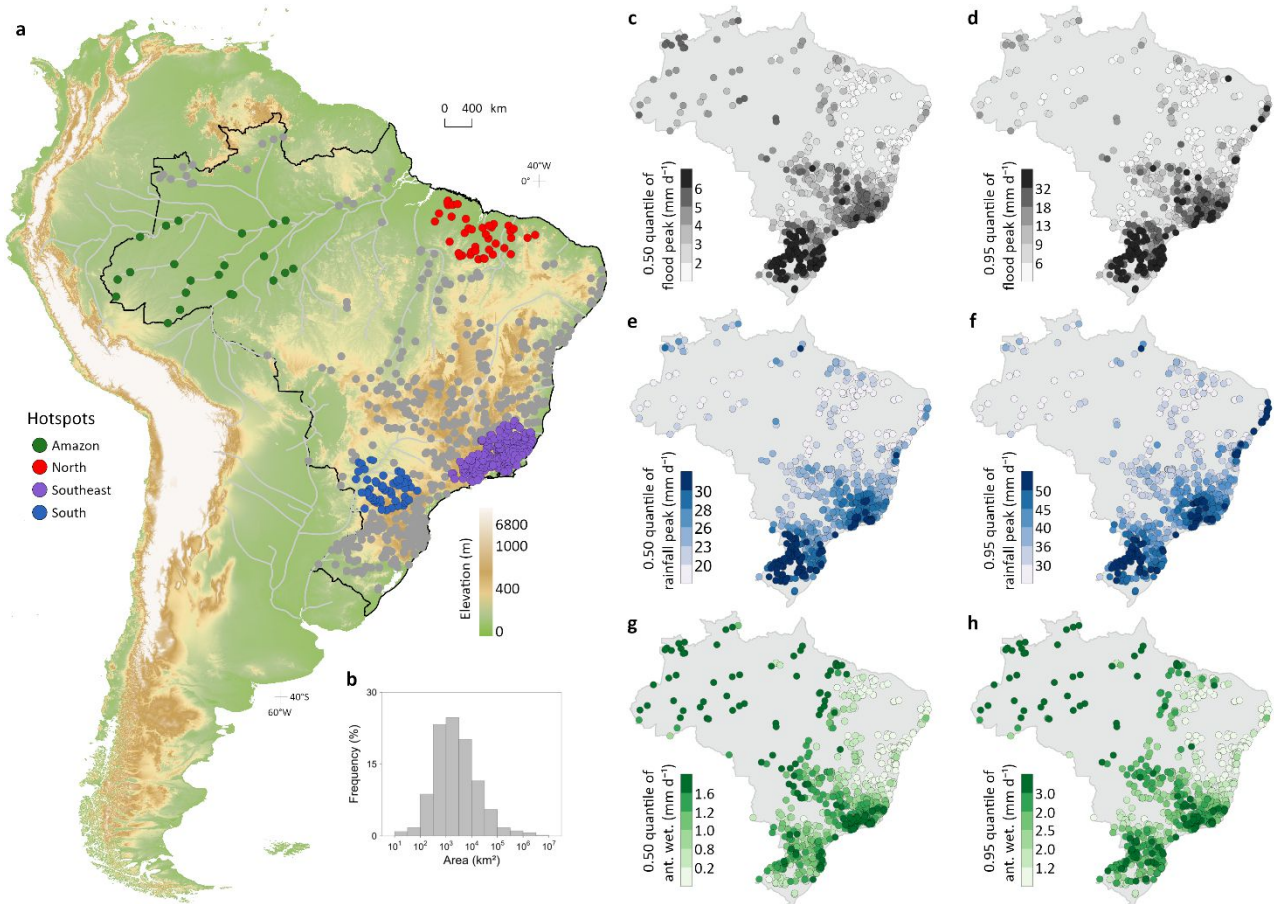


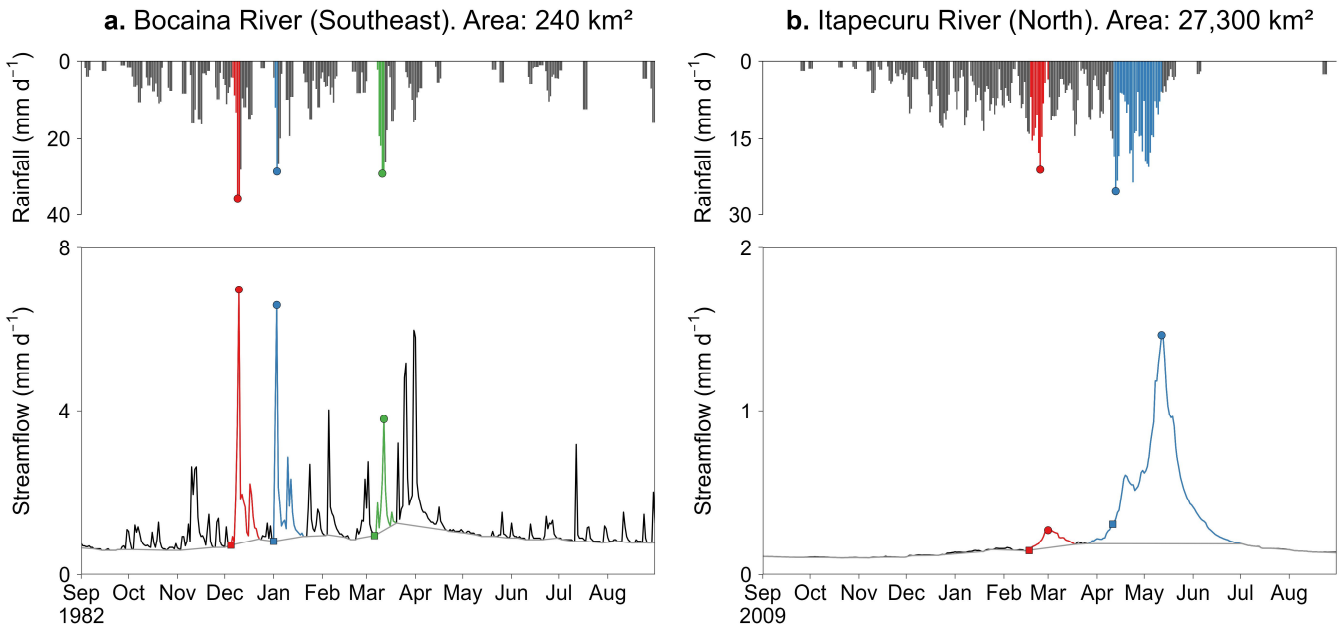
Figure 1. (a) South American topography (in meters above the mean sea level) and location of the 765 catchments and four hotspots of change. The number of selected gauges in each hotspot is: 22 (Amazon), 40 (North), 181 (Southeast), 56 (South). (b) Frequency distribution of catchment area (log₁₀-scale). The black line indicates the territorial boundary of Brazil. Light grey lines show major rivers. (c) 0.50 quantile (median) of flood peak time series; (d) 0.95 quantile of flood peak time series; (e) 0.50 quantile of rainfall peak time series; (f) 0.95 quantile of rainfall peak time series; (g) 0.50 (median) quantile of antecedent wetness time series; (h) 0.95 quantile of antecedent wetness time series.



70 2.2 Flood event detection

The flood events are sampled based on rainfall magnitudes to ensure that the antecedent state of the catchments is independent of the flood response (Brunner et al., 2021; Ettrick et al., 1987; Wasko et al., 2021; Wasko and Nathan, 2019). Event sampling based on rainfall rather than flood magnitudes minimizes the bias in the catchment's antecedent state toward wet conditions. We identify flood events (Fig. 2) as follows. Independent streamflow events are extracted using a nonparametric baseflow separation method based on the identification of turning points in the daily streamflow time series (Institute of Hydrology, 1980). The procedure is as follows. First, local minima are identified within non-overlapping windows of size W days over the entire time series. Next, these local minima are filtered to select the turning points, defined as points with a streamflow at least 1.11 times smaller than that of their neighbouring points. Finally, baseflow is estimated by linearly interpolating between these turning points. The window size is estimated for each catchment as the breakpoint in the relationship between window size and the baseflow index by using segmented regression. After baseflow separation, independent events were identified from the streamflow time series by determining their start and end points. The start of an event is defined as the point when total runoff rises above baseflow, and the end is defined as when it reaches back to the baseflow level again. To avoid the detection of very small streamflow responses, only events with peak discharge higher than the long-term median streamflow are kept for further analysis. Additionally, to ensure a robust separation of streamflow events in large catchments, we visually inspect the identified events, and W values are manually adjusted if necessary.

The rainfall peak and the catchment antecedent wetness of each streamflow event are estimated based on the rising limb of the event hydrograph. Following Merz et al. (2018), we establish a maximum backward time window from the flood peak to ensure that the rainfall peak and antecedent wetness are truly relevant to flood peak generation. If the rising limb of the event exceeds 30 days, both rainfall peak and antecedent wetness are estimated using a fixed 30-day window from the flood peak. This decision is based on observations in large catchments where the rising limb of flood events can span a few months; rainfall peaks or antecedent wetness conditions from a few months before the flood peak may no longer be representative. The 30-day window is chosen because shorter time windows (e.g., 7 or 14 days) overestimate the antecedent wetness state in those large catchments. To ensure the robustness of our findings, we repeated the analysis without large catchments ($>50,000 \text{ km}^2$) and found that the conclusions remain unchanged (not shown).



95 **Figure 2. Example of rainfall-based peak-over-threshold flood event identification in two catchments with contrasting streamflow responses.** Streamflow and rainfall time series for (a) Bocaina River, a small catchment located in the Southeast hotspot, with a catchment area of 240 km^2 (gauge ID 58220000); (b) Itapecuru River, a large catchment located in the North hotspot, with a catchment area of $27,300 \text{ km}^2$ (gauge ID 33530000). The bars in the upper panels in (a-b) represent the rainfall time series, and the grey and black lines in the lower panels indicate the estimated baseflow and observed streamflow time series, respectively. The colors highlight the selected events. The circles indicate the rainfall and streamflow peaks; the squares in the lower panel represent the streamflow value at the start of the event hydrograph (i.e., the catchment antecedent wetness).

100 105 110 115

We assume that all rainfall (smoothed by a 3-day moving average) occurring within this rising limb contributes to streamflow generation. Ideally, this time window would be increased by the catchment response time to account for the delay between rainfall and streamflow response. However, this is challenging, as response time varies with event magnitude and empirical estimates can differ by up to 500% depending on the method used (Grimaldi et al., 2012). The catchment antecedent wetness is computed by using the pre-event streamflow value, i.e., the streamflow value one day before the start of the rising limb. We use the pre-event streamflow as a proxy for catchment antecedent wetness state because it is widely used as a wetness indicator (e.g., Ettrick et al., 1987; Fischer & Schumann, 2025; Merz et al., 2018; Plate et al., 1988; Tarasova et al., 2018), can be easily derived from streamflow time series, relies on observational data rather than reanalysis-based soil moisture, and does not require the definition of additional parameters and assumptions such as antecedent precipitation index (Woldemeskel and Sharma, 2016). In the majority of catchments, the rainfall peak corresponds to the highest rainfall within the hydrograph's rising limb, and the pre-event streamflow reflects baseflow conditions (see circles and squares in Fig. 2a). However, in large catchments where the rising limb extends beyond 30 days, both the rainfall peak and antecedent wetness are estimated based on the constrained 30-day time window (e.g., Fig. 2b). Lastly, we sample the flood events with a frequency-based rainfall



peak-over-threshold approach. Only events with rainfall peaks above a threshold that ensures, on average, three events per year are kept in the sample. For instance, in a time series with 30 years of data, we sampled the largest 90 rainfall peaks.

2.3 Detection and attribution of flood change

We use quantile regression (Koenker, 2005) for the detection and attribution of flood changes. Quantile regression allows us to explore changes and their drivers in both the center and tail of the flood statistical distribution. We focus on two quantiles of interest: the 0.50 (median) quantile, which is a proxy for the median flood behavior or small flood events; and the 0.95 quantile, which is a proxy for large flood events. Fig. 1c-1h shows the 0.50 and 0.95 quantiles of flood peak, rainfall peak, and antecedent wetness time series.

For the detection of change, we assume a log-linear dependency between the target variable (y) and time (t , in days). We estimate the τ -th conditional quantile of y , $Q(\log_{10}(y_i) | \tau)$, as:

$$Q(\log_{10}(y_i) | \tau) = \alpha^{(\tau)} + \beta_{t,y}^{(\tau)} t_i + \varepsilon_i^{(\tau)}, \quad (1)$$

in which y is target variable – flood peak (q), rainfall peak (r), or antecedent wetness (w); τ is the quantile of interest; $\alpha^{(\tau)}$ and $\beta_{t,y}^{(\tau)}$ are the intercept and slope of the linear time-dependent model; and $\varepsilon_i^{(\tau)}$ is the error component (residuals). The slope parameter is the estimated trend, which is transformed into percentage per decade as follows:

$$\delta_y^{(\tau)} = 100 \left(10^d \beta_{t,y}^{(\tau)} - 1 \right), \quad (2)$$

in which d is the number of days in one decade.

For the attribution model, we analyze the interannual variability of flood peaks and drivers in a multivariate framework. We assume a log-log dependence of flood peaks with rainfall peaks (r) and antecedent wetness (w) to estimate the τ -th conditional quantile of flood peaks, $Q(\log_{10}(q_i) | \tau)$:

$$Q(\log_{10}(q_i) | \tau) = \alpha^{(\tau)} + \beta_r^{(\tau)} \log_{10}(r_i) + \beta_w^{(\tau)} \log_{10}(w_i) + \varepsilon_i^{(\tau)}, \quad (3)$$

in which $\beta_r^{(\tau)}$ and $\beta_w^{(\tau)}$ are the intercept and slopes of the linear attribution model. The log-log regression allows us to interpret the model coefficients as elasticities, meaning they represent the percentage change in flood peaks resulting from a 1% change in one of the drivers. For example, a 1% increase in rainfall peak would lead to $\beta_r^{(\tau)}\%$ increase in flood peak magnitude, assuming that antecedent wetness remains unchanged. We estimate the contribution of each driver of flood change in absolute and relative terms in a similar fashion to Bertola et al. (2021). The contribution of each driver is estimated by multiplying its elasticity (Eq. 3) by the change in the driver (Eq. 1) of the corresponding quantile, enabling us to explore the underlying relationship between changes in flood and drivers at different magnitudes (i.e., 0.50 and 0.95 quantiles). Assuming that the



contribution of the drivers is additive, we estimate the relative contribution of each driver as the ratio between its absolute contribution and the sum of the absolute values of the individual contributions of all drivers. Since correlations between drivers
145 and their underlying trends can introduce bias in the interpretation of the results, we check for these correlations. Rainfall peak and antecedent wetness are weakly correlated, with a median Spearman correlation of 0.04. Likewise, the trends in rainfall peak and antecedent wetness show only a weak relationship, with Spearman correlation of 0.004 for the 0.50-quantile trends and -0.02 for the 0.95-quantile trends.

The flood magnitudes are expected to follow the variations in their drivers. For instance, increasing flood magnitudes can be
150 attributed to increasing extreme rainfall, whereas decreasing rainfall cannot reasonably cause increasing floods (which would imply a negative elasticity). Therefore, we follow Bertola et al. (2021) and apply a parameter constraint for the attribution model to prevent negative elasticity values, ensuring a hydrologically reasonable relationship between floods and their drivers and a straightforward interpretation of the results. We found negative elasticities in only 0.3 and 4.4% of the catchments for small and large events, respectively, indicating that most catchments have hydrologically consistent relationships between
155 floods and their drivers.

The significance of the model parameters is assessed using robust covariance matrix estimators at a 5% local significance level, which accounts for potential heteroscedasticity, autocorrelation, and non-normality of the residuals. In addition, we employ the False Discovery Rate (FDR; Benjamini & Hochberg, 1995) to address the overestimation of significant results when conducting multiple statistical tests across different catchments (Wilks, 2016), to assess field significance (Renard et al.,
160 2008), and to ensure a robust analysis of spatially dependent variables (Wilks, 2006). We follow the suggestion of Wilks (2016) for highly dependent data in space and assume an FDR-adjusted significance level of two times the local significance level (i.e., $\alpha_{FDR} = 10\%$).



3 Results

165 3.1 Detection of change

Small and large flood events have been changing differently in Brazil (Fig. 3 and 4). Trends in small flood events (Fig. 3a) are overwhelmingly negative across Brazil, with 70.2% of the catchments showing decreasing magnitudes. The observed changes in small flood events range from -48.4 to +50% per decade, with a median value of -4.5% per decade. Out of the 765 catchments, 17.3% showed statistically significant changes ($\alpha_{FDR} = 10\%$), 3.5 times higher than the expected 5% local significance level. In contrast, changes in large floods (Fig. 3b) showed a higher proportion of catchments experiencing increasing magnitudes (43.5%) compared to small floods. Changes in large floods range from -76.6 to +59.2% per decade, with a median trend of -1.8% per decade. We observed a 2.7 times larger-than-expected proportion of statistically significant changes ($\alpha_{FDR} = 10\%$) in large floods (i.e., 13.7%). Large events are increasing more (or decreasing less) than small events, as 78% of substantial flood increases (exceeding 13.5% per decade threshold, defined as a one standard deviation of the flood 170 change distribution) are observed in large events (Fig. 4b; trend differences are shown in Fig. S1).

Remarkable differences in changes in small and large floods are observed in the Southeast and South hotspots, where most small floods are decreasing in magnitude (median trend of -2.4 and -6% per decade, respectively) and large floods are increasing (both with median trend close to +3% per decade). In the North hotspot, small floods are decreasing at higher rates than large floods (median trends of -9.4 and -4.2% per decade). In the Amazon hotspot, small and large floods are increasing 180 similarly (median trends of 2.1 and 2.6% per decade, respectively).

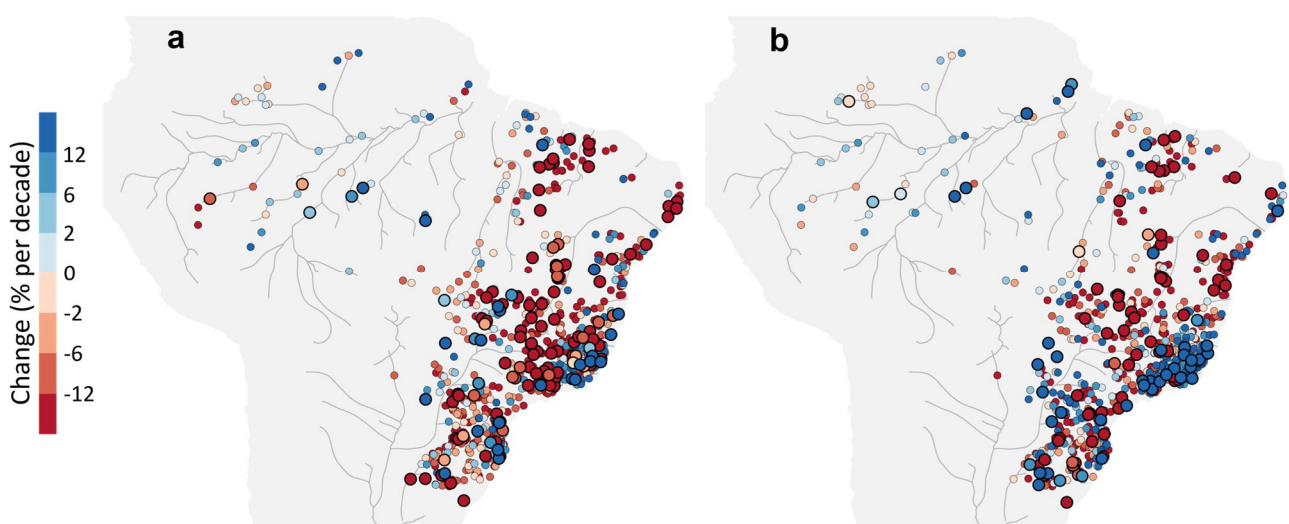
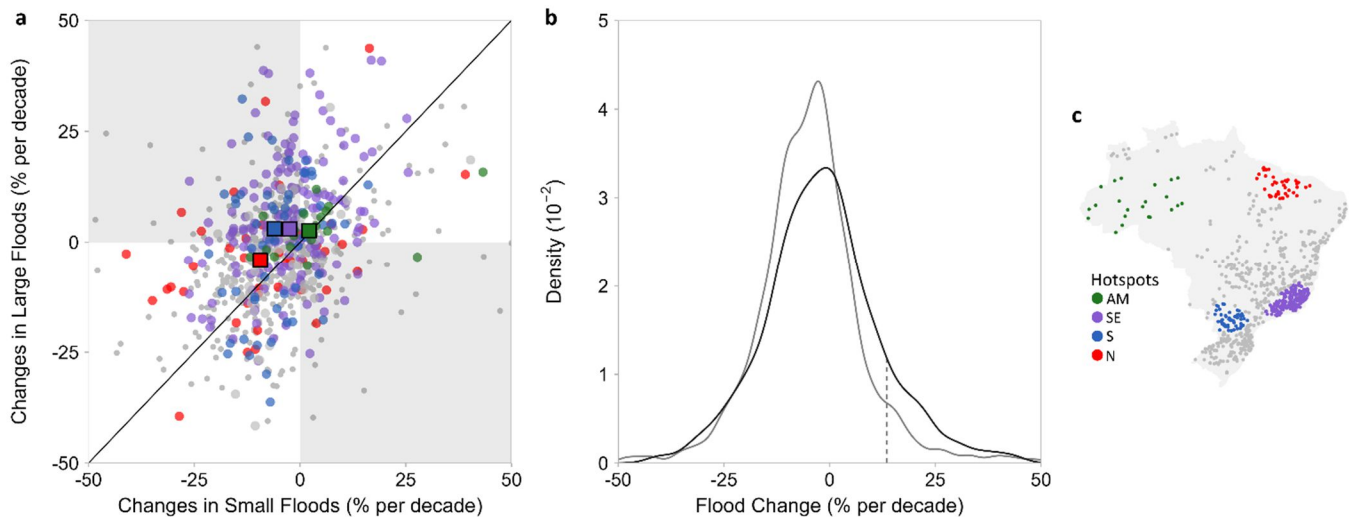


Figure 3. Estimated changes, in % per decade, for (a) small and (b) large flood events. Large circles with thick borders in (a-b) indicate statistical significance at an FDR-adjusted significance level ($\alpha_{FDR} = 10\%$).



185 **Figure 4.** (a) Relationship between changes, in % per decade, for small and large flood events for all catchments, classified according to five Brazilian hotspots. The points represent the local estimates of flood changes, and the squares represent the median of each hotspot. The black line represents the 1:1 function. (b) Empirical distribution of changes in small (gray) and large (black) events. The dashed line indicates one standard deviation derived from the pooled distribution of changes in small and large events. (c) Brazilian hotspots.

190 **3.2 Elasticity of floods to drivers**

To understand the sensitivity of floods to their drivers, we evaluate the elasticities of floods to rainfall peak and antecedent wetness (Fig. 5). Elasticity to rainfall peak is statistically significant ($\alpha_{FDR} = 10\%$) in a large proportion of catchments, i.e., 74 and 45% for small and large events, respectively. The elasticity of small floods to rainfall peak (Fig. 5a) is mostly high in Brazil, with median elasticities ranging between 0.24 to 1.6% across hotspots. Higher values are observed in the South and Southeast hotspots (median elasticity of 1.6 and 1.4%, respectively), and lower values in the Amazon and Northern regions (median elasticity ranging between 0.24 to 0.93%). Similar elasticities to rainfall peaks are observed for large events (Fig. 5b), with higher values observed in the South, Southeast, and North regions, with median elasticity ranging between 0.9 to 1.4%, and lower values in the Amazon (0.24%) region. These results suggest that, on average, the elasticity of floods to rainfall peak shows low dependence on event magnitude.

200 The elasticity of floods to antecedent wetness is notably lower than that to rainfall peaks, with median values ranging from 0.43 to 0.63% for small floods and from 0.27 to 0.46% for large floods across hotspots. Elasticity to antecedent wetness is statistically significant ($\alpha_{FDR} = 10\%$) in 77 and 39% for small and large events, respectively. Overall, higher elasticities to antecedent wetness are found in the Amazon (median elasticity of 0.50 and 0.35% to small and large events, respectively) and North (0.63 and 0.46%) hotspots. In contrast to the low dependence of rainfall peak elasticity to event magnitude, the elasticity of floods to antecedent wetness notably decreases with increasing event magnitude.

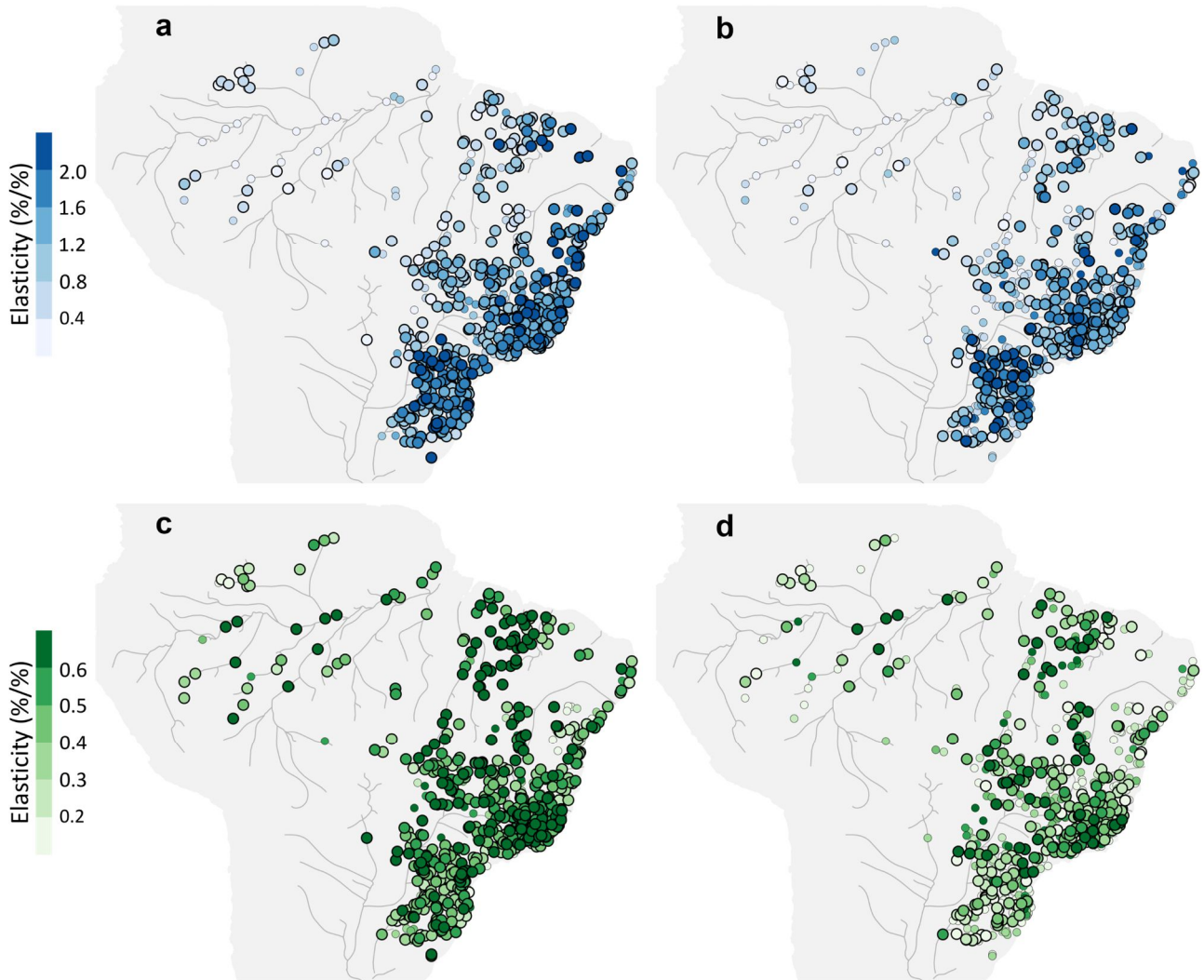


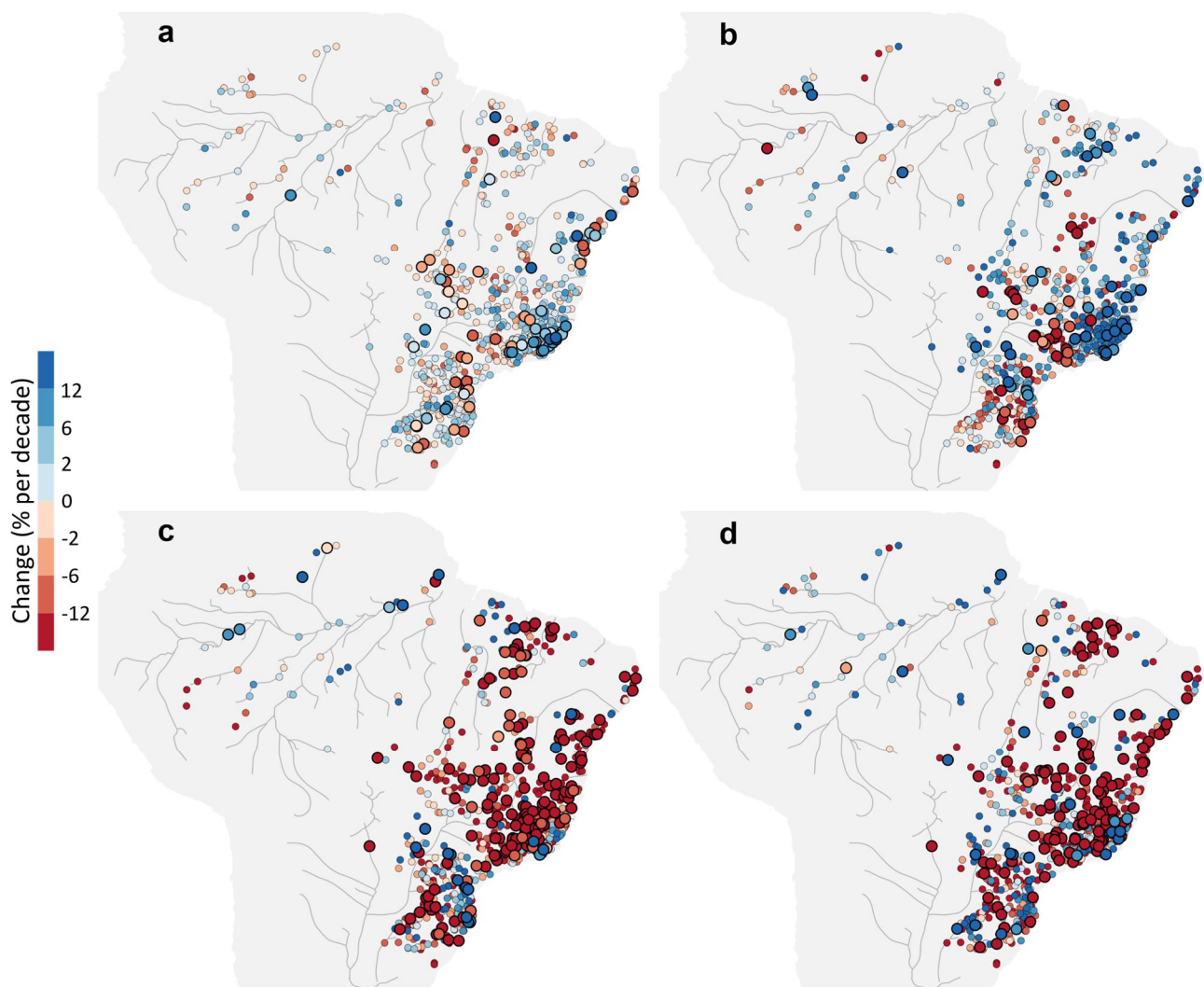
Figure 5. Estimated elasticities of floods to their drivers. (a-b) Elasticity of flood to rainfall peak for (a) small and (b) large events. (c-d) As in (a-b), but for the elasticity of flood to antecedent wetness. Large circles with thick borders in (a-d) indicate significance at an FDR-adjusted significance level ($\alpha_{FDR} = 10\%$). Please note the difference in scales between panels (a-b) and (c-d).

210 3.3 Attribution of flood changes

We contrast the flood changes with changes in rainfall peak and antecedent wetness (Fig. 6), allowing us to investigate the interplay of changes in small and large floods with different levels of rainfall extremeness (i.e., small and large rainfall peaks) and catchment states (i.e., dry or wet conditions). Rainfall peak (Fig. 6a and 6b) is mostly increasing in magnitude across Brazil, mainly in the Southeast and South regions. The spatial pattern of the sign of rainfall peak changes is quite similar for 215 small and large events in most hotspots, but the absolute magnitude notably increases for large events. In the North region,



there is a notable shift in the sign of rainfall changes (from negative to positive) between small and larger events. In contrast, antecedent wetness is decreasing in most of Brazil (Fig. 6c and 6d), except in parts of the South, Amazon, and Southeast hotspots, where antecedent wetness is increasing. The change pattern of antecedent wetness is quite similar in sign and magnitude for small and large quantiles.



220

Figure 6. Estimated changes of flood drivers, in % per decade. (a-b) Changes in rainfall peaks for (a) small and (b) large events. (c-d) as in (a-b), but for antecedent wetness. Large circles with thick borders in (a-d) show significance at an FDR-adjusted significance level ($\alpha_{FDR} = 10\%$).

Our results can be further understood by looking at the relative contribution of flood change that is explained by changes in
225 each driver (Fig. 7 and Fig. S2), which combines both flood elasticities and trends in drivers of change. For small floods (Fig.



7a), flood changes are more linked with antecedent wetness than with rainfall peak in 69.8% of the catchments, especially in the Amazon (median relative contribution of 80%), North (82%), and Southeast (64%), with low to moderate contributions of rainfall peak – relative contribution of rainfall peak is up to 36%. In the South hotspot, despite the higher median contribution of antecedent wetness (60%), there is substantial overlap with the relative contribution of rainfall peak, suggesting that the
230 dominant driver varies considerably across catchments.

For large floods, the importance of rainfall peak increases, where flood changes are more linked with rainfall peak than antecedent wetness changes in 58.8% of the catchments. We find a clear shift in the driving mechanisms of flood change for large events in Southeast and South hotspots (Fig. 7b), where flood change becomes rainfall-driven, with median relative contributions of 68% and 64%, respectively. In the other hotspots, the dominant driving mechanism is still antecedent wetness,
235 i.e., Amazon (median relative contribution of 58%) and North (63%). However, there are higher contributions of rainfall peak compared with the small events, whereas the relative contribution is up to 42%.

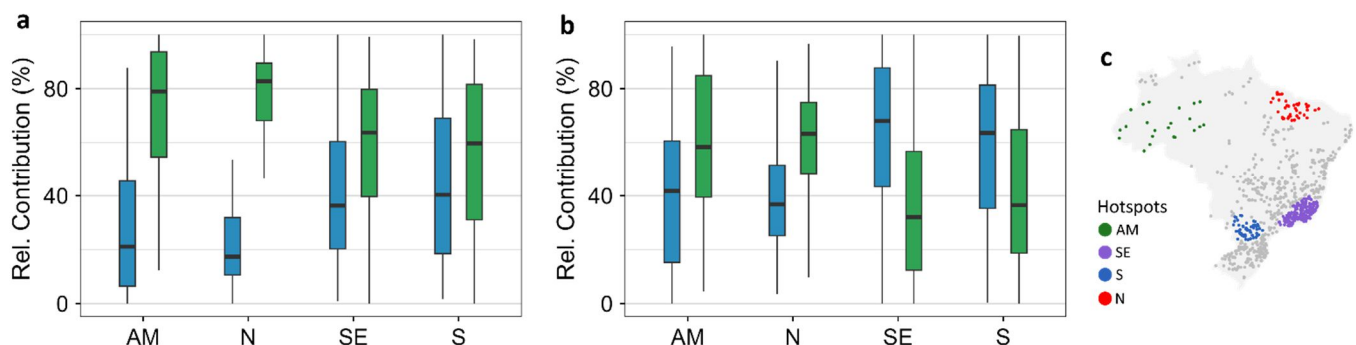


Figure 7. Estimated relative contributions of drivers to small and large flood events. Relative contribution of rainfall peak (blue) and antecedent wetness (green) to flood changes for: (a) small events; and (b) large events. (c) Brazilian hotspots.

240 **4. Discussion**

4.1 Change patterns across small and large floods

Most of our observed changes in the average floods using peak-over-threshold sampling are aligned with previous findings using maximum annual floods in Brazil. Decreasing flood magnitudes are observed in most of Brazil, with increasing flood magnitudes only in the Amazon and along the Southeast coast (e.g., Anzolin et al., 2023; Bartiko et al., 2019; Berghuijs et al.,
245 2016; Chagas et al., 2022; Do et al., 2017; Gudmundsson et al., 2019; Petry et al., 2025; Slater et al., 2021; Souza & Reis, 2022). The change pattern in the Amazon region shows good agreement with several regional assessments, which further support the observed increases in flood magnitude (e.g., Barichivich et al., 2018; Espinoza et al., 2022; Espinoza Villar et al., 2009; Gloor et al., 2013) and floodplain inundation (e.g., Fleischmann et al., 2023). However, some differences in flood patterns are particularly evident in Southern Brazil, where annual maximum floods are mostly increasing (Bartiko et al., 2017;



250 Chagas and Chaffe, 2018). The differences we found may be attributed to our event extraction strategy, which uses a rainfall-based peak-over-threshold sampling instead of relying on the maximum annual streamflow series. The reasoning is that not every intense rainfall leads to a large flood response and, by analyzing events with smaller flood magnitudes compared with maximum annual streamflow, different patterns are likely to be observed (Ettrick et al., 1987; Sharma et al., 2018). These results highlight the importance of assessing flood change patterns using a broader range of events, rather than relying solely
255 on annual maximum time series. Changes in large floods have been timidly explored in Brazil so far (e.g., Chagas et al., 2024), mostly by global-scale assessments with fewer catchments included in the dataset (Wasko et al., 2021). Good agreements of changes in large floods were found with a rainfall-based peak-over-threshold approach (Wasko et al., 2021), even for a different sampling frequency (i.e., on average 5 events per year) and data period (1948–2014).

260 Changes in large flood events are not well correlated with changes in small floods in Brazil, with a Spearman correlation coefficient of 0.38 (p-value < 0.001). This noticeable difference can be easily observed by inspection of the spatial pattern (Fig. 3a and 3b) and the scatterplot (Fig. 4a), which do not follow the 1:1 line. Differences in flood patterns of small and large floods have also been observed in the United States (Slater & Villarini, 2016), with Spearman correlation of 0.49 between action floods (events requiring mitigation action in preparation for more substantial flooding) and major floods (events with extensive inundation, significant evacuations, or property transfer), defined based on US National Weather Service (NOAA
265 National Weather Service, 2012) guidelines. In Australia (Wasko & Nathan, 2019), and globally (Wasko et al., 2021). Less pronounced differences are found in Europe (Bertola et al., 2020), with a Spearman correlation of 0.79 between the annual 2-year and 100-year floods. This high correlation between changes in small and large events can be partly attributed to the model structure used for trend estimation (Merz et al., 2021). The regional nonstationary frequency model relies on the widely used index flood methodology (Hosking and Wallis, 1997), in which the estimated trend in the 100-year flood depends on the 2-
270 year flood trend.

4.2 Hydrological mechanisms of flood change

275 We find a dichotomous relationship between changes in rainfall peak and flooding. Despite the increases in rainfall peak, such increases do not always translate into increased flooding. In fact, changes in rainfall peak alone do not explain the spatial variability of flood change in many parts of Brazil, especially for small flood events. Such differences between rainfall peak and flood changes can be partly attributed to changes in antecedent wetness conditions, where decreasing antecedent wetness outweighs the rainfall increases. This is supported by evidence that rising temperatures are likely to intensify rainfall extremes (Berg et al., 2013; Trenberth, 2011) and increase drought periods (Dai, 2013), consequently reducing soil moisture at the onset of extreme rainfall events and leading to decreases in flood magnitudes even under increased rainfall (Sharma et al., 2018). This dichotomous relationship has been found in several regions worldwide, where extreme rainfall events are increasing
280 globally (Alexander et al., 2006; Donat et al., 2013; Papalexiou and Montanari, 2019; Sun et al., 2021; Wasko et al., 2021; Westra et al., 2013), whereas floods remain unchanged or do not necessarily follow the rainfall increases



(Bartiko et al., 2019; Bertola et al., 2020; Blöschl et al., 2019; Kemter et al., 2023; Wasko et al., 2021; Wasko and Nathan, 2019).

We find two main patterns of flood changes and driving mechanisms in Brazil. In some regions, changes in small and large 285 floods are relatively consistent in sign and are both more associated with changes in antecedent wetness. In other parts of Brazil, we observe a regional shift in the sign of flood change and its driving mechanisms, where small floods are more linked with antecedent wetness and the large ones are more rainfall-driven. We hypothesize that the regional differences between changes in small and large floods and their driving mechanism are linked with catchment responsiveness, which we interpret in terms of catchment water storage capacities, as previously described for flood-generating mechanisms in Brazil (Chagas et 290 al., 2022a). The first pattern we found, i.e., a similar flood pattern (in terms of sign) and driving mechanisms between small and large floods is more frequently observed in regions with high water storage capacity, such as the Amazon and North regions. In these regions, several land surface attributes control catchments' responsiveness, including deep and highly 295 permeable soils (Hengl et al., 2017), low topographic slopes, and the formation of extensive floodplains and wetlands (Fleischmann et al., 2023), making these catchments less sensitive to rainfall changes. The second pattern we found, i.e., different change patterns and driving mechanisms between small and large floods is more often observed in regions with low water storage capacity, such as the South and Southeast regions. In these regions, land surface attributes are characterized by higher topographic slopes, mountain ranges, and shallower soils (Hengl et al., 2017), making these catchments more sensitive to rainfall changes.

5 Conclusions

300 Here, we explore the causes of changes in small and large flood events by combining flood elasticities with trends in rainfall and antecedent wetness of 765 catchments in Brazil. For each catchment, we select flood peaks, their corresponding rainfall and antecedent wetness using a frequency-based peak-over-threshold approach. Our results suggest that increasing magnitudes are more often observed for large floods, where 80% of substantial flood increases are observed in large events. Changes in small floods are more linked with antecedent wetness than with extreme rainfall in 70% of the study area, while 305 changes in large events are more rainfall-driven (59%). We found two main patterns of flood change mechanisms across Brazil, which we hypothesize are linked to catchment responsiveness, interpreted here in terms of water storage capacity. In regions with high water storage capacity, antecedent wetness drives flood change in both small and large events. Conversely, in regions with low water storage capacity, changes in small events are driven by antecedent wetness, while changes in large floods are mainly rainfall-driven. Our findings highlight that reliable predictions of flood responses to climate change should account for 310 both event magnitude and catchment storage capacities, as climatic drivers alone are insufficient to fully explain flood changes, particularly in regions with high storage capacities.



Conflict of Interest. The authors declare no conflicts of interest relevant to this study.

Author Contributions. All co-authors designed the overall study. GA performed the analysis and prepared the paper. All co-
315 authors contributed to the interpretation of the results and writing of the paper.

Data Availability. Daily streamflow and rainfall data are available at <https://doi.org/10.5281/zenodo.3709337>.

Acknowledgments. This work was supported by the Coordination for the Improvement of Higher Education Personnel (CAPES) and the Brazilian National Council for Scientific and Technological Development (CNPq).

References

320 Alexander, L. V., Zhang, X., Peterson, T. C., Caesar, J., Gleason, B., Klein Tank, A. M. G., Haylock, M., Collins, D., Trewin, B., Rahimzadeh, F., Tagipour, A., Rupa Kumar, K., Revadekar, J., Griffiths, G., Vincent, L., Stephenson, D. B., Burn, J., Aguilar, E., Brunet, M., Taylor, M., New, M., Zhai, P., Rusticucci, M., and Vazquez-Aguirre, J. L.: Global observed changes in daily climate extremes of temperature and precipitation, *Journal of Geophysical Research: Atmospheres*, 111, <https://doi.org/10.1029/2005JD006290>, 2006.

325 Anzolin, G., Chaffee, P. L. B., Vrugt, J. A., and AghaKouchak, A.: Using climate information as covariates to improve nonstationary flood frequency analysis in Brazil, *Hydrological Sciences Journal*, 68, 645–654, <https://doi.org/10.1080/02626667.2023.2182212>, 2023.

330 Barichivich, J., Gloor, E., Peylin, P., Brien, R. J. W., Schöngart, J., Espinoza, J. C., and Pattnayak, K. C.: Recent intensification of Amazon flooding extremes driven by strengthened Walker circulation, *Sci Adv*, 4, <https://doi.org/10.1126/sciadv.aat8785>, 2018.

Bartiko, D., Chaffee, P. L. B., and Bonumá, N. B.: Nonstationarity in maximum annual daily streamflow series from Southern Brazil, *RBRH*, 22, <https://doi.org/10.1590/2318-0331.0217170054>, 2017.

Bartiko, D., Oliveira, D. Y., Bonumá, N. B., and Chaffee, P. L. B.: Spatial and seasonal patterns of flood change across Brazil, *Hydrological Sciences Journal*, 64, 1071–1079, <https://doi.org/10.1080/02626667.2019.1619081>, 2019.

335 Benjamini, Y. and Hochberg, Y.: Controlling the False Discovery Rate: A Practical and Powerful Approach to Multiple Testing, *J R Stat Soc Series B Stat Methodol*, 57, 289–300, <https://doi.org/10.1111/j.2517-6161.1995.tb02031.x>, 1995.

Berg, P., Moseley, C., and Haerter, J. O.: Strong increase in convective precipitation in response to higher temperatures, *Nat Geosci*, 6, 181–185, <https://doi.org/10.1038/ngeo1731>, 2013.



Berghuijs, W. R., Woods, R. A., Hutton, C. J., and Sivapalan, M.: Dominant flood generating mechanisms across the United
340 States, *Geophys Res Lett*, 43, 4382–4390, <https://doi.org/10.1002/2016GL068070>, 2016.

Bertola, M., Viglione, A., and Blöschl, G.: Informed attribution of flood changes to decadal variation of atmospheric, catchment and river drivers in Upper Austria, *J Hydrol (Amst)*, 577, 123919, <https://doi.org/10.1016/j.jhydrol.2019.123919>, 2019.

Bertola, M., Viglione, A., Lun, D., Hall, J., and Blöschl, G.: Flood trends in Europe: are changes in small and big floods
345 different? *Hydrol Earth Syst Sci*, 24, 1805–1822, <https://doi.org/10.5194/hess-24-1805-2020>, 2020.

Bertola, M., Viglione, A., Vorogushyn, S., Lun, D., Merz, B., and Blöschl, G.: Do small and large floods have the same drivers of change? A regional attribution analysis in Europe, *Hydrol Earth Syst Sci*, 25, 1347–1364, <https://doi.org/10.5194/hess-25-1347-2021>, 2021.

Blöschl, G., Hall, J., Viglione, A., Perdigão, R. A. P., Parajka, J., Merz, B., Lun, D., Arheimer, B., Aronica, G. T., Bilibashi,
350 A., Boháč, M., Bonacci, O., Borga, M., Čanjevac, I., Castellarin, A., Chirico, G. B., Claps, P., Frolova, N., Ganora, D., Gorbachova, L., Gül, A., Hannaford, J., Harrigan, S., Kireeva, M., Kiss, A., Kjeldsen, T. R., Kohnová, S., Koskela, J. J., Ledvinka, O., Macdonald, N., Mavrova-Guirguinova, M., Mediero, L., Merz, R., Molnar, P., Montanari, A., Murphy, C., Osuch, M., Ovcharuk, V., Radevski, I., Salinas, J. L., Sauquet, E., Šraj, M., Szolgay, J., Volpi, E., Wilson, D., Zaimi, K., and Živković, N.: Changing climate both increases and decreases European river floods, *Nature*, 573, 108–111,
355 <https://doi.org/10.1038/s41586-019-1495-6>, 2019.

Brunner, M. I., Swain, D. L., Wood, R. R., Willkofer, F., Done, J. M., Gilleland, E., and Ludwig, R.: An extremeness threshold determines the regional response of floods to changes in rainfall extremes, *Commun Earth Environ*, 2, 173, <https://doi.org/10.1038/s43247-021-00248-x>, 2021.

Chagas, V. B. P. and Chaffé, P. L. B.: The Role of Land Cover in the Propagation of Rainfall Into Streamflow Trends, *Water
360 Resour Res*, 54, 5986–6004, <https://doi.org/10.1029/2018WR022947>, 2018.

Chagas, V. B. P., L. B. Chaffé, P., Addor, N., M. Fan, F., S. Fleischmann, A., C. D. Paiva, R., and Siqueira, V. A.: CAMELS-BR: Hydrometeorological time series and landscape attributes for 897 catchments in Brazil, *Earth Syst Sci Data*, 12, 2075–2096, <https://doi.org/10.5194/essd-12-2075-2020>, 2020.

Chagas, V. B. P., Chaffé, P. L. B., and Blöschl, G.: Climate and land management accelerate the Brazilian water cycle, *Nat
365 Commun*, 13, <https://doi.org/10.1038/s41467-022-32580-x>, 2022b.

Chagas, V. B. P., Chaffé, P. L. B., and Blöschl, G.: Process Controls on Flood Seasonality in Brazil, *Geophys Res Lett*, 49, <https://doi.org/10.1029/2021GL096754>, 2022a.



Chagas, V. B. P., Chaffé, P. L. B., and Blöschl, G.: Drought-Rich Periods Are More Likely Than Flood-Rich Periods in Brazil, *Water Resour Res*, 60, <https://doi.org/10.1029/2023WR035851>, 2024.

370 370 Dai, A.: Increasing drought under global warming in observations and models, *Nat Clim Chang*, 3, 52–58, <https://doi.org/10.1038/nclimate1633>, 2013.

Do, H. X., Westra, S., and Leonard, M.: A global-scale investigation of trends in annual maximum streamflow, *J Hydrol (Amst)*, 552, 28–43, <https://doi.org/10.1016/j.jhydrol.2017.06.015>, 2017.

375 375 Donat, M. G., Alexander, L. V., Yang, H., Durre, I., Vose, R., Dunn, R. J. H., Willett, K. M., Aguilar, E., Brunet, M., Caesar, J., Hewitson, B., Jack, C., Klein Tank, A. M. G., Kruger, A. C., Marengo, J., Peterson, T. C., Renom, M., Oria Rojas, C., Rusticucci, M., Salinger, J., Elrayah, A. S., Sekele, S. S., Srivastava, A. K., Trewin, B., Villarroel, C., Vincent, L. A., Zhai, P., Zhang, X., and Kitching, S.: Updated analyses of temperature and precipitation extreme indices since the beginning of the twentieth century: The HadEX2 dataset, *Journal of Geophysical Research: Atmospheres*, 118, 2098–2118, <https://doi.org/10.1002/jgrd.50150>, 2013.

380 380 Espinoza, J.-C., Marengo, J. A., Schongart, J., and Jimenez, J. C.: The new historical flood of 2021 in the Amazon River compared to major floods of the 21st century: Atmospheric features in the context of the intensification of floods, *Weather Clim Extrem*, 35, 100406, <https://doi.org/10.1016/j.wace.2021.100406>, 2022.

385 385 Espinoza Villar, J. C., Guyot, J. L., Ronchail, J., Cochonneau, G., Filizola, N., Fraizy, P., Labat, D., de Oliveira, E., Ordoñez, J. J., and Vauchel, P.: Contrasting regional discharge evolutions in the Amazon basin (1974–2004), *J Hydrol (Amst)*, 375, 297–311, <https://doi.org/10.1016/j.jhydrol.2009.03.004>, 2009.

Ettrick, T. M., Mawdsey, J. A., and Metcalfe, A. V.: The influence of antecedent catchment conditions on seasonal flood risk, *Water Resour Res*, 23, 481–488, <https://doi.org/10.1029/WR023i003p00481>, 1987.

Fischer, S. and Schumann, A. H.: Dominant flood types in Europe and their role in flood statistics, *Hydrological Sciences Journal*, 1–17, <https://doi.org/10.1080/02626667.2025.2450369>, 2025.

390 390 Fleischmann, A. S., Papa, F., Hamilton, S. K., Fassoni-Andrade, A., Wongchuig, S., Espinoza, J.-C., Paiva, R. C. D., Melack, J. M., Fluet-Chouinard, E., Castello, L., Almeida, R. M., Bonnet, M.-P., Alves, L. G., Moreira, D., Yamazaki, D., Revel, M., and Collischonn, W.: Increased floodplain inundation in the Amazon since 1980, *Environmental Research Letters*, 18, 034024, <https://doi.org/10.1088/1748-9326/acb9a7>, 2023.

395 395 Funk, C., Peterson, P., Landsfeld, M., Pedreros, D., Verdin, J., Shukla, S., Husak, G., Rowland, J., Harrison, L., Hoell, A., and Michaelsen, J.: The climate hazards infrared precipitation with stations—a new environmental record for monitoring extremes, *Sci Data*, 2, 1–21, <https://doi.org/10.1038/sdata.2015.66>, 2015.



Gloor, M., Brienen, R. J. W., Galbraith, D., Feldpausch, T. R., Schöngart, J., Guyot, J. -L., Espinoza, J. C., Lloyd, J., and Phillips, O. L.: Intensification of the Amazon hydrological cycle over the last two decades, *Geophys Res Lett*, 40, 1729–1733, <https://doi.org/10.1002/grl.50377>, 2013.

400 Grimaldi, S., Petroselli, A., Tauro, F., and Porfiri, M.: Time of concentration: a paradox in modern hydrology, *Hydrological Sciences Journal*, 57, 217–228, <https://doi.org/10.1080/02626667.2011.644244>, 2012.

Gudmundsson, L., Leonard, M., Do, H. X., Westra, S., and Seneviratne, S. I.: Observed Trends in Global Indicators of Mean and Extreme Streamflow, *Geophys Res Lett*, 46, 756–766, <https://doi.org/10.1029/2018GL079725>, 2019.

405 Gudmundsson, L., Boulange, J., Do, H. X., Gosling, S. N., Grillakis, M. G., Koutoulis, A. G., Leonard, M., Liu, J., Müller Schmied, H., Papadimitriou, L., Pokhrel, Y., Seneviratne, S. I., Satoh, Y., Thiery, W., Westra, S., Zhang, X., and Zhao, F.: Globally observed trends in mean and extreme river flow attributed to climate change, *Science* (1979), 371, 1159–1162, <https://doi.org/10.1126/science.aba3996>, 2021.

410 Hengl, T., Mendes de Jesus, J., Heuvelink, G. B. M., Ruiperez Gonzalez, M., Kilibarda, M., Blagotić, A., et al.: SoilGrids250m: Global gridded soil information based on machine learning, *PLOS ONE*, 12, e0169748, doi:10.1371/journal.pone.0169748, 2017.

Hosking, J. R. M. and Wallis, J. R.: Regional Frequency Analysis, Cambridge University Press, <https://doi.org/10.1017/CBO9780511529443>, 1997.

Institute of Hydrology: Low flow studies, Report No. 1, Wallingford, UK, 1980.

415 Kemter, M., Marwan, N., Villarini, G., and Merz, B.: Controls on Flood Trends Across the United States, *Water Resour Res*, 59, <https://doi.org/10.1029/2021WR031673>, 2023.

Koenker, R.: Quantile Regression, Cambridge University Press, Cambridge, 349 pp., 2005.

Merz, B., Dung, N. V., Apel, H., Gerlitz, L., Schröter, K., Steirou, E., and Vorogushyn, S.: Spatial coherence of flood-rich and flood-poor periods across Germany, *J Hydrol (Amst)*, 559, 813–826, <https://doi.org/10.1016/j.jhydrol.2018.02.082>, 2018.

420 Merz, B., Blöschl, G., Vorogushyn, S., Dottori, F., Aerts, J. C. J. H., Bates, P., Bertola, M., Kemter, M., Kreibich, H., Lall, U., and Macdonald, E.: Causes, impacts and patterns of disastrous river floods, *Nat Rev Earth Environ*, 2, 592–609, <https://doi.org/10.1038/s43017-021-00195-3>, 2021.



Minasny, B. and Hartemink, A. E.: Predicting soil properties in the tropics, *Earth Sci Rev*, 106, 52–62, <https://doi.org/10.1016/j.earscirev.2011.01.005>, 2011.

NOAA National Weather Service: NWS Manual 10-950. Definitions and General Terminology, Hydrological Services
425 Program, NWSPD, 10-9, 2012.

Papalexiou, S. M. and Montanari, A.: Global and Regional Increase of Precipitation Extremes Under Global Warming, *Water Resour Res*, 55, 4901–4914, <https://doi.org/10.1029/2018WR024067>, 2019.

Petry, I., Miranda, P. T., Paiva, R. C. D., Collischonn, W., Fan, F. M., Fagundes, H. O., Araujo, A. A., and Souza, S.: Changes
430 in Flood Magnitude and Frequency Projected for Vulnerable Regions and Major Wetlands of South America, *Geophys Res Lett*, 52, <https://doi.org/10.1029/2024GL112436>, 2025.

Plate, E. J., Ihringer, J., and Lutz, W.: Operational models for flood calculations, *J Hydrol (Amst)*, 100, 489–506, [https://doi.org/10.1016/0022-1694\(88\)90198-9](https://doi.org/10.1016/0022-1694(88)90198-9), 1988.

Renard, B., Lang, M., Bois, P., Dupeyrat, A., Mestre, O., Niel, H., Sauquet, E., Prudhomme, C., Parey, S., Paquet, E., Neppel, L., and Gailhard, J.: Regional methods for trend detection: Assessing field significance and regional consistency, *Water Resour
435 Res*, 44, <https://doi.org/10.1029/2007WR006268>, 2008.

Sharma, A., Wasko, C., and Lettenmaier, D. P.: If Precipitation Extremes Are Increasing, Why Aren't Floods?, *Water Resour Res*, 54, 8545–8551, <https://doi.org/10.1029/2018WR023749>, 2018.

Slater, L., Villarini, G., Archfield, S., Faulkner, D., Lamb, R., Khouakhi, A., and Yin, J.: Global Changes in 20-Year, 50-Year, and 100-Year River Floods, *Geophys Res Lett*, 48, 1–10, <https://doi.org/10.1029/2020GL091824>, 2021.

440 Slater, L. J. and Villarini, G.: Recent trends in U.S. flood risk, *Geophys Res Lett*, 43, <https://doi.org/10.1002/2016GL071199>, 2016.

Souza, S. A. de and Reis, Jr., D. S.: Trend Detection in Annual Streamflow Extremes in Brazil, *Water (Basel)*, 14, 1805, <https://doi.org/10.3390/w14111805>, 2022.

Sun, Q., Zhang, X., Zwiers, F., Westra, S., and Alexander, L. V.: A Global, Continental, and Regional Analysis of Changes in
445 Extreme Precipitation, *J Clim*, 34, 243–258, <https://doi.org/10.1175/JCLI-D-19-0892.1>, 2021.

Tarasova, L., Basso, S., Zink, M., and Merz, R.: Exploring Controls on Rainfall-Runoff Events: 1. Time Series-Based Event Separation and Temporal Dynamics of Event Runoff Response in Germany, *Water Resour Res*, 54, 7711–7732, <https://doi.org/10.1029/2018WR022587>, 2018.



Trenberth, K. E.: Changes in precipitation with climate change, *Clim Res*, 47, 123–138, <https://doi.org/10.3354/cr00953>, 2011.

450 Wasko, C. and Nathan, R.: Influence of changes in rainfall and soil moisture on trends in flooding, *J Hydrol (Amst)*, 575, 432–441, <https://doi.org/10.1016/j.jhydrol.2019.05.054>, 2019.

Wasko, C., Nathan, R., Stein, L., and O’Shea, D.: Evidence of shorter more extreme rainfalls and increased flood variability under climate change, *J Hydrol (Amst)*, 603, 126994, <https://doi.org/10.1016/j.jhydrol.2021.126994>, 2021.

455 Westra, S., Alexander, L. V., and Zwiers, F. W.: Global Increasing Trends in Annual Maximum Daily Precipitation, *J Clim*, 26, 3904–3918, <https://doi.org/10.1175/JCLI-D-12-00502.1>, 2013.

Wilks, D. S.: On “Field Significance” and the False Discovery Rate, *J Appl Meteorol Climatol*, 45, 1181–1189, <https://doi.org/10.1175/JAM2404.1>, 2006.

Wilks, D. S.: "The Stippling Shows Statistically Significant Grid Points": How Research Results are Routinely Overstated and Overinterpreted, and What to Do about It, *Bull. Am. Meteorol. Soc.*, 97, 2263–2273, doi:10.1175/BAMS-D-15-00267.1, 2016.

460 Wohl, E., Barros, A., Brunsell, N., Chappell, N. A., Coe, M., Giambelluca, T., Goldsmith, S., Harmon, R., Hendrickx, J. M. H., Juvik, J., McDonnell, J., and Ogden, F.: The hydrology of the humid tropics, *Nat Clim Chang*, 2, 655–662, <https://doi.org/10.1038/nclimate1556>, 2012.

Woldemeskel, F. and Sharma, A.: Should flood regimes change in a warming climate? The role of antecedent moisture conditions, *Geophys Res Lett*, 43, 7556–7563, <https://doi.org/10.1002/2016GL069448>, 2016.

465